Water-Related Adsorbates on Stepped Platinum Surfaces

Kolb, Manuel Jerome

Chapter 2

Density Functional Theory Study of Adsorption of H_2O, H, O and OH on Stepped Platinum Surfaces

2.1 Abstract

We report on DFT-GGA-computed adsorption energetics of water and the water-related fragments OH, O and H on stepped Pt surfaces in the low coverage limit. The Pt(100) step edge as encountered on Pt(533) shows increased binding for all species studied, while the Pt(110) step edge, as found on Pt(553) shows only significantly enhanced binding for O and OH. Comparing these results to ultra-high-vacuum experiments reveals that DFT can explain the main experimental trends semiquantitatively.

Published as: Manuel J. Kolb, Federico Calle-Vallejo, Ludo B.F. Juurlink and Marc T.M. Koper, The Journal of Chemical Physics, 140, 134708, 2014

2.2 Introduction

Platinum plays a key role in catalysis, and it is ideally suited as electrocatalyst for low-temperature Polymer Electrolyte Membrane (PEM) fuel cells,[1] water electrolysis and many other electrochemical reactions. Understanding the interaction between platinum surfaces and water molecules at the atomic level is important for the further improvement of its activity and in creating new, cost-effective catalysts that perform similarly to platinum [2, 3]. In order to achieve a complete picture of real catalytic surfaces, which usually consist of small particles on a support, not only the consideration of high-symmetry facets of the surface is required, but also the influence of step and kink sites on adsorption and reactivity [4, 5]. The effect of isolated step sites can be systematically studied using regularly stepped surfaces. These consist of flat terraces of high-symmetry facets interrupted by mono-atomic steps. This setup allows for direct observation of the influence of the step type on the reactivity, thereby providing some insight on the influence of steps on the overall catalytic activity. Traditionally, most experimental and theoretical studies devoted to the interaction of water with platinum surfaces have dealt with either flat Pt(111) surfaces or other facets with rather low surface indices [6, 7]. While this helps to reduce computational efforts, such calculations give limited insight into the adsorption energies of isolated steps due to the influence of step-step interactions and the interactions between all terrace adsorption sites with the step edge on short terraces. However, more recent computational studies [8–10] have considered surfaces with steps of a separation distance similar to the one studied in this paper.

In previous experimental work from our group [11], we studied the desorption of H, O and H_2O from two stepped Pt surfaces, Pt(533) and Pt(553), using the Temperature Programmed Desorption (TPD) technique in ultra-high vacuum (UHV). The Pt(533) surface consists of a 4-atom-long terrace of (111) character and a (100) step edge, whereas the Pt(553) surface has a 5-atom-long (111) terrace and a (111) step edge. A side- and top-view of the surfaces are shown further into the paper as figures 2.1 and 2.2.

It was found that hydrogen desorbs in a two-peak structure from Pt(533) and in a more complicated pattern with two or three peaks from Pt(553). Atomic oxygen was found to desorb in a two-peak structure from both surfaces. The high-temperature peak was found at higher temperatures for Pt(533) compared to Pt(553) [11]. Desorption of H_2O was observed to exhibit a three-peak structure for both Pt(533) and Pt(553). The low-energy peak was assigned to multi-layer desorption. The high-energy peak was attributed to desorption from steps, since it was not observed on the flat Pt(111) surface. The intermediate-temperature peak was located at a temperature comparable to that of Pt(111), therefore it

was assigned to desorption from terraces. The high-temperature peak was detected at comparable temperatures for both surfaces, suggesting that the adsorption energies of water for the two different step geometries are not significantly different. For most adsorbates it was concluded that step sites should bind adsorbates stronger than terrace sites, and for H and O this tendency is stronger for the (100)-type step site. For a more detailed description of the desorption spectra we refer to the original publication.

The aim of this study is to establish a qualitative explanation for the results of the TPD experiments, by computing the adsorption energy of water and its dissociation products H, O and OH on the stepped surfaces Pt(533) and Pt(553) using Density Functional Theory. This will serve as a benchmark for future studies on the interaction of water with adsorbate-covered stepped Pt surfaces and complements other studies on the intrinsic different catalytic acivity of (100) and (110) step edges [12].

2.3 Computational

The computations were performed using the ab-initio density functional code VASP [13–16] using the PBE exchange-correlation functional [17] and PAW potentials [18, 19]. The PBE functional was chosen in order to obtain reasonable adsorption energies across the whole range of species studied here to and adequately describe hydrogen bonding among water molecules [20] for future calculations that include solvation. The k-point sampling was done using a Monkhorst - Pack scheme [21] using 9x9x1 sampling for the Pt(111) surface and a 3x9x1 sampling for the stepped Pt(533) and Pt(553) surfaces. A basis set with a cut-off energy of 550 eV was chosen. For all calculations first-order Methfessel-Paxton smearing [22] with a sigma of 0.2 was applied and all energies were extrapolated to an electronic temperature of 0 K. All calculations were performed spin restricted. The replicated images of the cells due to the periodic boundary conditions were separated by about 20 Å of vacuum. Gas phase species were calculated using a 10x10x10 Å unit cell with a 1x1x1 k-point sampling in which the gas phase species were placed.

The Pt(111) surface was a 2x2 replicated surface unit cell with 3 relaxing layers at the top and 2 layers fixed at bulk positions at the bottom. This is beyond what is necessary for convergence on a (111) surface, but proved necessary to achieve consistency with the stepped surfaces. Figures 2.1a) and 2.1b) show a side view of the model stepped surfaces. Fixed layers are black, surface layers are silver, the first subsurface layer is blue and the second subsurface layer is red. Note that when using a 4-layer model to stepped surfaces the atom that forms the lower

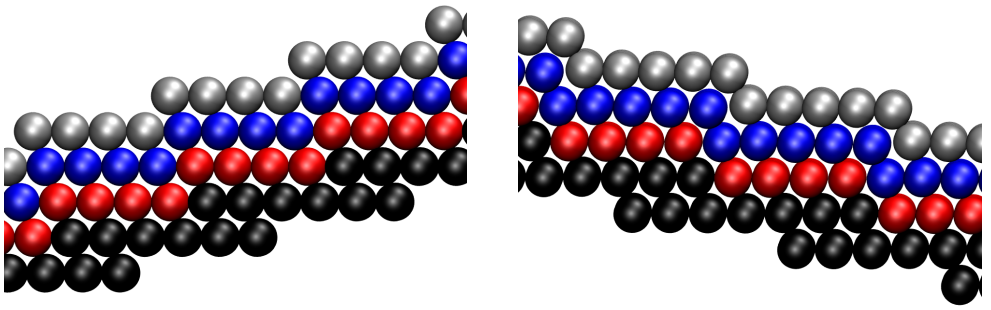

(a) Pt(533) (b) Pt(553)

Figure 2.1: Sideview of the two model surfaces

step edge has a nearest neighbor that is fixed in its bulk position, resulting in a distorted step edge. This influences the total energy for that cell and the resulting step geometry. Therefore, we increased the number of layers to 5 to solve this problem. The resulting unit cell was then replicated in the direction parallel to the step edge to achieve similar adsorbate-adsorbate separation as on Pt(111). The free energies of adsorption of H, O, OH and H_2O were calculated as follows:

$$\Delta G_{ads,H} = G_{total,H_{ads}} - G_{clean} - \frac{1}{2}G_{H_2(g)} \tag{2.1}$$

$$\Delta G_{ads,O}^{O_2(g)} = G_{total,O_{ads}} - G_{clean} - \frac{1}{2}G_{O_2(g)} \tag{2.2a}$$

where,

$$G_{O_2(g)} = 2(G_{H_2O(g)} - G_{H_2} - \Delta G_{form,exp}^{H_2O}) \tag{2.2b}$$

and

$$\Delta G_{form,exp}^{H_2O}(g) = -2.37\ eV\ at\ P = 1\ atm\ and\ T = 298.15\ K \tag{2.2c}$$

$$\Delta G_{ads,O}^{H_2O} = G_{total,O_{ads}} - G_{clean} - G_{H_2O}(g) + G_{H_2(g)} \tag{2.3}$$

$$\Delta G_{ads,OH} = G_{total,OH_{ads}} - G_{clean} - G_{H_2O}(g) + \frac{1}{2}G_{H_2(g)} \tag{2.4}$$

$$\Delta G_{ads,H_2O} = G_{total,H_2O_{ads}} - G_{clean} - G_{H_2O(g)} \tag{2.5}$$

Each individual G was calculated as follows:

$$G_{A_{ads}} = E_{DFT,A} + ZPE(A) - T * S(A)_{vib} \tag{2.6}$$

for adsorbate A and

$$G_{B(g)} = E_{DFT,B} + ZPE(B) - T * S(B) \tag{2.7}$$

for gas-phase species B. Note that S(B) is the total entropy and is taken from reference tables for gas phase species [23].

The free energies of adsorption of oxygen were calculated for two references (Eq. 2.2a and 2.3). One for comparison to gas phase O_2 (Eq. 2.2a) which is the more relevant reference for comparison to TPD experiments, that is calculated based on the experimental formation energy of water (Eq. 2.2b), in order to avoid the inaccuracy of the DFT value for O_2 [24, 25]. The other reference is calculated using water as a reference (Eq. 2.3), which is the relevant reference value for comparison to electrochemistry and for the possible formation of OH on step edges. All adsorption energies below are Gibbs energies and corrected for zero-point energy (ZPE) and vibrational entropy at 298 K, following the methods described by Loffreda [26].

The adsorption sites on Pt(533) and Pt(553) surfaces are illustrated in figures 2.2a and 2.2b. Platinum atoms in the surface layer are colored in silver, those in the subsurface layer are blue and those in the second layer below the surface are red. The adsorption sites are OT for on-top adsorption, B for bridge sites and FCC/HCP for the two three-fold hollow adsorption sites. Bronze bonds represent the direct connection between two surface atoms in the (111) plane, magenta bonds show direct connections in the (100)/(110) steps. A full catalogue of adsorption sites, their associated energies, vibrational frequencies and geometry information is available in the supporting information [27].

2.4 Results and Discussion

2.4.1 The Pt(533) and Pt(553) surfaces

In the absence of adsorbates, the surface relaxation is not extensive, i.e. the displacements of edge atoms are quite small. The total energy gained from relaxing the top three layers of the surface is small (0.0122 and 0.0076 eV per platinum atom in the unit cell for Pt(533) and Pt(553), respectively). In both optimized structures the exposed surface area is minimized by retracting the edge atoms into the deeper layers, as can be seen in figures 2.1a and 2.1b. These relaxation effects on edge atoms lead to a slight tilt of the (111) surface towards the (533)/(553) surface normal.

Adsorption energies on the stepped surfaces are not completely converged with respect to the thickness of the slab. However, tests showed that this leads to a

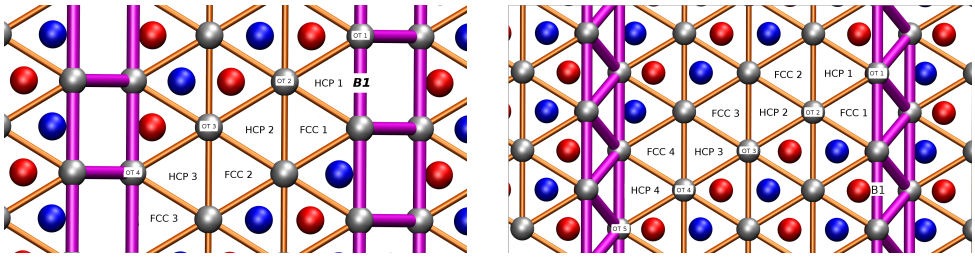

(a) Pt(533) (b) Pt(553)

Figure 2.2: Adsorption sites on the stepped surfaces (Surface layer atoms marked silver, second layer atoms blue and third layer atoms red)

uniform shift of the adsorption energies of all sites. The results of these tests can be found in the supporting information. This allows us to look primarily at general trends in adsorption energies. We emphasize that the simultaneous full convergence of all adsorption energies for all species on all surfaces considered here is not within the scope of this paper. In order to observe possible trends in the shift of the d-band center for the step-edge atoms, the LDOS (local density of states) for the surface atoms of the Pt(111) facet and step edge atoms of the two studied surfaces were calculated and can be found in the supporting information. No obvious shift or difference in the d-band center for either surface was observed.

2.4.2 Hydrogen Adsorption

The distinct adsorption sites for hydrogen are the on-top position, the bridge position between two surface platinum atoms and the two three-fold hollow sites, HCP and FCC. These adsorption sites are, from an energetic point of view, almost equivalent, with a slight preference towards the three-fold hollow sites. The results for Pt(111) using our approach can be found in table 2.1. Earlier results obtained by Olsen et al. [28] with two different GGA functionals (BP and PW91) revealed a similar range of adsorption energies as computed here. The functionals in those studies however showed a clear trend towards on-top adsorption, which is not found here. It should be noted that the results of Olsen et al. did not take ZPE and vibrational entropy into account, so they cannot be directly compared to the Gibbs energies of adsorption computed here.

For the stepped surfaces almost all bridge sites on the terrace do not contribute to adsorption, because the two neighboring three-fold hollow sites are, unlike on the flat Pt(111) surface, no longer equivalent in energy. This leads to an energy gradient that moves the hydrogen atom out of the bridge position towards the

Table 2.1: Adsorption energies for hydrogen on Pt(111), Pt(533) and Pt(553)

Adsorption Site	$G_{Pt(111)}[eV]$	$G_{Pt(533)}[eV]^*$	$G_{Pt(553)}[eV]^*$
OT terrace (OT2/OT3)	-0.26	-0.20	-0.18
HCP terrace (HCP2/HCP3)	-0.26	-0.18	-0.15
FCC terrace (FCC2/FCC3)	-0.29	-0.21	-0.21
Bridge terrace	-0.25	—	—
Bridge B1	—	-0.41	-0.26
On-Top OT1	—	-0.26	-0.19
FCC1	—	-0.19	-0.28
HCP1	—	-0.23 **	-0.28
On-Top OT4 / OT5	—	-0.27	-0.16

* Adsorption energy converged to 0.05eV for present layer thickness (see SI)

** Approximate energy, atom fixed at unstable adsorption site

neighboring site with the strongest binding. In table 2.1 we only provide the adsorption sites in the middle of the terrace for comparison to pristine Pt(111). A full overview of all adsorption sites can be found in the supporting information.

On the Pt(533) surface, the strongest binding site is the B1 site on the step edge. The OT1 site, which is also located on the step edge, shows enhanced binding compared to the OT site on the terrace as well. However, the nearby B1 site is significantly more stable, therefore on real surfaces this site will probably not play a role. Another binding site is the OT4, which is located on the lower step edge and also shows slightly enhanced binding compared to Pt(111). It should be noted that this site has a two-fold coordination, despite being identified as an on-top site, since it is also located close to the platinum atom in the upper step edge. The three-fold hollow sites on the step edge, named FCC1 and HCP1, show binding energies comparable to the FCC1 site on the Pt(533) terrace, although the HCP1 site is no longer stable and hydrogen will move to the B1 site with no noticeable barrier. To estimate the energy of this binding site the atom was fixed at the HCP1 site, which then showed slightly enhanced binding compared to the terrace, even in this unrelaxed HCP position. On the Pt(553) surface the situation is significantly different. The most important sites on the surface are again shown in table 2.1. We found that B1 on the step edge of this surface binds hydrogen significantly weaker than the same site on the Pt(533) step edge. The B1 site is therefore no longer the strongest binding site, but is energetically comparable

Table 2.2: Adsorption energies for oxygen on Pt(111), Pt(533) and Pt(553)

Adsorption Site	$G_{O_{ad},Pt(111)}$ [eV] $^{+}$	$G_{O_{ad},(533)}$ [eV] $^{*+}$	$G_{O_{ad},(553)}$ [eV] $^{*+}$
On-Top, terrace	0.14 / 2.51	0.42 / 2.79	0.43 / 2.79
HCP hollow ,terrace	-0.68 / 1.69	-0.62 / 1.75	-0.57 / 1.80
FCC hollow, terrace	-1.14 / 1.23	-0.96 / 1.41	-0.92 / 1.45
Bridge B1	—	-1.43 / 0.94	-1.10 / 1.27
FCC1	—	-1.07 / 1.30	-1.29 / 1.08
OT5	—	—	-0.91 / 1.46

* Adsorption energy converged to within 0.05 eV for present layer thickness (see SI)

$^{+}$ First value for O_2(g) reference, second for H_2O reference

to the FCC1 position. The lower step edge on Pt(553) also binds hydrogen significantly weaker than the comparable geometry on Pt(533). The terrace sites, however, show very similar binding energies as the Pt(533) terraces. This means that the most important difference between the Pt(553) and the Pt(533) surfaces is the stronger stabilization provided by the Pt(533) step edge.

Comparison to Experiment

In the temperature-programmed desorption experiments of van der Niet et al. [11], desorption of deuterium was compared on Pt(111), Pt(533) and Pt(553). They found that the introduction of steps only leads to stabilization of H on the Pt(533) step edge and not on Pt(553). Our DFT findings are in good agreement with those results. Reproducing the details of the TPD spectra requires a more detailed account of lateral interactions and surface diffusion, as presented in [29, 30].

2.4.3 Oxygen Adsorption

In order to ensure consistency with previous results (e.g. [31]), we will briefly discuss the results for oxygen adsorption on Pt(111). We find that the FCC site is the most stable, with an adsorption energy of -1.14 eV with respect to the O_2(g) reference or 1.23 eV on the H_2O-based scale. This is followed by the HCP site and the on-top site. The bridge position is, in contrast to hydrogen, unstable and leads to a shift into one of the hollow sites. It should be noted that our results are all obtained using non-spin-polarized calculations, leading to a slightly

underestimated binding for the on-top site, as can be expected due to an increased net spin of the bonded oxygen when performing spin-polarized calculations.[32]. We find an energy difference between spin-restricted and unrestricted calculations of about 0.1 eV for the on-top site, while no changes are observed for any site with an oxygen atom that is coordinated to more than one platinum atom. None of the affected sites plays a role in the actual adsorption since even their corrected adsorption energies are well above all neighboring sites.

On the stepped Pt(533) surface the situation is similar to the case of hydrogen discussed earlier. The binding energies for the most important sites can be found in table 2.2. The B1 site again shows enhanced binding compared to the Pt(111) surface, although we find no stable binding site on the lower step edge as we did for hydrogen. The FCC1 site on the upper step edge shows an adsorption energy that is comparable to the FCC site on the Pt(111) surface. On the Pt(553) surface the results are again notably different. The strongest adsorption site is now the FCC1 site on the upper step edge, comparable to the case for hydrogen. Additionally, the OT5 site, which actually has three-fold coordination due to its position on the lower edge of the step, is able to bind oxygen.

In conclusion, our calculations for oxygen adsorption on stepped platinum surfaces show that the strongest binding would occur at the B1 position on Pt(533), which binds oxygen significantly stronger than on Pt(111). On Pt(553) we find an increased binding compared to Pt(111) but this increase is less than on Pt(533).

Comparison to Experiment

Van der Niet et al. found in their TPD study that oxygen desorbing from Pt(533) shows a two-peak structure with a peak at 774 K and another one at 663 K[11]. The low-temperature peak was found at a comparable temperature as desorption from Pt(111) and was, therefore, assigned to desorption from terraces. The high-temperature peak was assigned to oxygen desorption from steps. On Pt(553) they found a similar two-peak structure, however the high-energy peak was located at the somewhat lower temperature of 738 K. This suggests that the step edge in Pt(533) binds oxygen stronger than Pt(111) terraces and also stronger than the Pt(553) step edge. This matches satisfactorily our DFT results. The change of the preferred adsorption site from the B1 site on the step edge for Pt(533) to the FCC1 site behind the step edge is in agreement with the results observed by DFT(LDA) and STM in the study by Feibelman et al. [33].

Table 2.3: Adsorption energies for H_2O on Pt(111), Pt(533) and Pt(553), most stable geometries at the given points

Adsorption Site	$G_{Pt(111)}$ [eV]	$G_{Pt(533)}[eV]$ *	$G_{Pt(553)}[eV]$ *
On-Top, terrace, flat	0.28	0.27	0.24
OT1, step edge	—	0.06	0.07

* Adsorption energy converged to within 0.05 eV for present layer thickness (see SI)

2.4.4 H_2O Adsorption

For Pt(111) we find an adsorption energy for water monomers adsorbed in a flat on-top position of 0.28 eV. This value differs significantly from earlier studies, none of which included both ZPE and vibrational entropy. Our raw DFT energy E, -0.23 eV is closer to the literature results of -0.30 eV calculated with PW91 [34, 35]. The Gibbs energy of water adsorption is rather sensitive to the actual observed geometry of adsorption. The actual value for vibrational entropy changes by as much as 30 % when rotating the water molecule at a certain site. Nevertheless, this only changes the adsorption energy by about 0.05 eV at most, and therefore the general trends detailed here are still expected to be valid. For the sake of consistency, in the following we will continue using the same convention as before and provide the Gibbs energies of adsorption at 298K. Due to this convention most adsorption energies will be positive, which is intuitively expected, because water will have desorbed from the surface long before reaching that temperature [11]. We also note that for water the convergence with regard to the number of layers is faster than for oxygen and hydrogen.

The tendency of water to bind preferentially atop platinum atoms is still valid on the stepped surfaces. Table 2.3 contains the adsorption energies for the aforementioned Pt(111) surface and for both stepped surfaces. However, the on-top positions on the step edge bind water with a binding strength of 0.06 eV and 0.07 eV for the Pt(533) and Pt(553) surface respectively, compared to 0.28 eV for Pt(111). This is in qualitative agreement with earlier results for (100) and (110) step edges which showed an increase in binding energy E of ca. 0.15 eV for the step edge compared to flat Pt(111) surfaces [9].

Comparison to Experiment

In the TPD experiments performed by Van der Niet et al, it was found that water desorbs from stepped platinum surfaces in a three-peak structure[11]. The highest-temperature peak was always assigned to desorption from the step edges, since no comparable peak was observed on the Pt(111) surface. The desorption temperature for the step-related peak was found ca. 10K lower on the Pt(533) surface compared to the Pt(553) surface. The intermediate-temperature peak was assigned to desorption from terraces, since it agrees with the peak observed on Pt(111). The lowest-temperature peak was assigned to the desorption of water from multi-layer water structures. The DFT results presented here show qualitative agreement with experiment in that the terrace adsorption energy is lower than the adsorption energy on the step edge. It should be noted that the difference in adsorption energies for Pt(533) and Pt(553) observed experimentally is not explained by the present calculations of the adsorption of single water molecules.

2.4.5 OH Adsorption

As *OH* is an important water-related intermediate at electrochemical interfaces, we also provide adsorption energies for *OH* on the three surfaces. Pt(111) shows a large preference to adsorb the *OH* molecule in either an atop or a bridge position. The FCC and HCP hollows show significantly reduced binding energies. Adsorption energy values for *OH* on Pt(111) can be found in table 2.4. Our values are in agreement with the results by Nørskov and Campbell et al. [36] for the Pt(111) surface, who reported an adsorption energy of -1.54 eV against a gas-phase *OH* reference. Using their formation energy for gas-phase *OH* of 0.32 eV and transforming it to our energy reference yields an adsorption energy of +1.12 eV for the OH adsorption on Pt(111). Our adsorption energy value with ZPE correction but without vibrational entropy for the isolated *OH* molecule on the Pt(111) surface is 0.91 eV, which is reasonably close given that different functionals were used. Introducing steps into the surface breaks the symmetry of the adsorption sites in one direction of the surface. FCC and HCP hollow sites are not found to be local minima near step edges, suggesting that on Pt(111) they were mainly stabilized into a meta-stable position by the symmetry of the surface. The Pt(533) surface shows an increased binding at the step-edge bridge site, similar as for the other adsorbates. Additionally, we found a difference in the adsorption energy for the terrace bridge sites depending on their orientation. Bridge sites at the terraces of Pt(533) parallel to the step edge were found to be no longer stable near the step edge, while all other bridge sites were stable, although they show decreased binding compared to Pt(111). The binding energy on the step edge of Pt(553) is

Table 2.4: Adsorption energies for OH on Pt(111), Pt(533) and Pt(553)

Adsorption Site	$G_{Pt(111)}[eV]$	$G_{Pt(533)}[eV]$ *	$G_{Pt(553)}[eV]$ *
On-Top, terrace, flat	1.02	1.16	1.18
Bridge, terrace (parallel)	1.02 **	1.08	1.22
Bridge, terrace (other dir.)	1.02 **	1.23	1.16
Bridge B1	—	0.27	0.66
HCP hollow ,terrace	1.54	unstable	unstable
FCC hollow, terrace	1.27	unstable	1.44

* Adsorption energy converged to within 0.05 eV for present layer thickness (see SI)

** No directional influence on the Pt(111) surface

significantly less favorable compared to the Pt(533) surface. The bridge sites on the Pt(553) terrace show no directional variance with respect to binding energy, and all of them are stable. In conclusion, OH prefers to bind to step edges in the B1 position on both surfaces and is ca. 0.7 eV more stable for Pt(533) and ca. 0.4 eV for Pt(553) compared to Pt(111).

Comparison to Experiment

The adsorption of OH cannot be directly studied in UHV. Typically the generation of OH_{ads} is performed by dosing water onto a Pt surface pre-covered with O_{ads}. This leads to the following net reaction:

$$H_2O_{\text{ads}} + O_{\text{ads}} \longrightarrow 2OH_{\text{ads}} \tag{1}$$

Our calculations suggest that this reaction is exothermic on the Pt(100) step, endothermic on the Pt(111) surface and almost thermoneutral for the step edge on Pt(553), with a ΔG of -0.49 eV at 298K for the Pt(533) surface, +0.52 eV for Pt(111) and -0.01 eV for the Pt(553) surface (see table 2.5). These numbers were calculated by considering all adsorbates in isolation on their most stable adsorption sites. No interaction with water was considered, which is certainly important when studying electrochemical reactions [37, 38]. From these results we can conclude that reaction 1 generates more OH_{ads} on the Pt(533) step compared to Pt(553). On Pt(111) this reaction should not take place if stabilizing effects are not accounted for. Surrounding water will play an important role in stabilizing OH adsorbates via hydrogen bonds [39].

Table 2.5: ΔG for reactions (1) and (2) on different surfaces at 298K

	$H_2O_{ads} + O_{ads} \longrightarrow 2OH_{ads}$ (Reaction 1)	$H_2O_{ads} \longrightarrow OH_{ads} + H_{ads}$ (Reaction 2)
Pt(111)	0.52	0.47
Pt(533)	-0.49	-0.23
Pt(553)	-0.01	0.33

Additionally, it is also possible that thermal dissociation of water can result in the formation of OH groups on the surface. For this we considered the following reaction:

$$H_2O_{ads} \longrightarrow OH_{ads} + H_{ads} \tag{2}$$

This reaction has a ΔG of -0.23 eV on Pt(533), +0.33 eV on Pt(553) and +0.47 eV on Pt(111) at 298K, again with all adsorbates binding to their most stable sites in complete isolation. The results suggest that on the step edge of Pt(553) reaction 2 is endothermic, while for the step edge of Pt(533) water has a thermodynamic tendency to dissociate. On Pt(111) reaction 2 will not take place without further stabilization of OH. In conclusion, it can be assumed that in the low coverage limit on the Pt(533) surface, water will dissociate into H and OH on steps, depending on the barrier of the dissociation reaction, whereas on the Pt(553) surface there is no driving force towards forming OH.

2.5 Conclusions

In this paper, we presented the DFT-GGA adsorption energetics of water and the water-related fragments OH, O and H on stepped Pt surfaces in the low coverage limit for comparison with experimental results on the same surface. The general trend indicates that the (100) step edge present in Pt(533) shows signifcantly enhanced binding for all studied species, while the (111)/(110) step edge present in Pt(553) shows no significant increase in binding energy for H, noticeable increases for O and OH, although less than the Pt(533) step edge, and similar increases for H_2O when compared to Pt(533). We would ascribe this stronger bonding of the (100) step to its more open character compared to the (111) step, though we note that there is no noticeable change in the local d-band center. Comparison of these results to experimental TPD measurements previously obtained in our group shows that the general trends of the low coverage results of the TPD measurements are matched by the calculations. Nevertheless, for the high coverage limit, as well

as for water and OH, where interactions between the adsorbates play a large role, trends may no longer be explained with the present results. The benchmark study presented here gives confidence that including interactions between adsorbates and water should yield valuable results that will improve the theoretical description of realistic platinum surfaces.

2.6 Acknowledgments

We gratefully acknowledge financial support from the Netherlands Organization for Scientific Research (NWO) as a TOP grant awarded to LBFJ and MTMK, and the National Research School Catalysis (NRSC). This work was sponsored also by the NWO Exacte Wetenschappen, EW (NWO Physical Sciences Division) for the use of supercomputer facilities, with financial support from the Nederlandse Organisatie voor Wetenschappelijk Onderzoek (Netherlands Organisation for Scientific Research, NWO).

References

(1) Gasteiger, H. A.; Kocha, S. S.; Sompalli, B.; Wagner, F. T. *Appl. Catal. B: Environmental* **2005**, *56*, 9 –35.

(2) Koper, M. T. M., *Fuel Cell Catalysis: A Surface Science Approach*; Wiley: 2009.

(3) Rabis, A.; Rodriguez, P.; Schmidt, T. J. *ACS Catalysis* **2012**, *2*, 864–890.

(4) Marković, N. M.; Ross, P. N. *Surf. Sci. Rep.* **2002**, *45*, 117 –229.

(5) Koper, M. T. M. *Nanoscale* **2011**, *3*, 2040–3364.

(6) Olsen, R.; Badescu, S.; Ying, S.; Baerends, E. *J. Chem. Phys.* **2004**, *120*, 11852–11863.

(7) Burch, R.; Daniells, S.; Breen, J.; Hu, P. *J. Catal.* **2004**, *224*, 252 –260.

(8) Rafti, M.; Vicente, J. L.; Albesa, A.; Scheibe, A.; Imbihl, R. *Surf. Sci.* **2012**, *606*, 12 –20.

(9) Arnadottir, L.; Stuve, E. M.; Jonsson, H. *Surf. Sci.* **2010**, *604*, 1978 –1986.

(10) Buso-Rogero, C.; Herrero, E.; Bandlow, J.; Comas-Vives, A.; Jacob, T. *Phys. Chem. Chem. Phys.* **2013**, *15*, 18671–18677.

(11) Van der Niet, M. J. T. C.; den Dunnen, A.; Juurlink, L. B. F.; Koper, M. T. M. *J. Chem. Phys.* **2010**, *132*, 174705.

(12) Tison, Y.; Nielsen, K.; Mowbray, D. J.; Bech, L.; Holse, C.; Calle-Vallejo, F.; Andersen, K.; Mortensen, J. J.; Jacobsen, K. W.; Nielsen, J. H. *J. Phys. Chem. C* **2012**, *116*, 14350–14359.

(13) Kresse, G.; Hafner, J. *Phys. Rev. B* **1993**, *47*, 558–561.

(14) Kresse, G.; Hafner, J. *Phys. Rev. B* **1994**, *49*, 14251–14269.

(15) Kresse, G.; Furthmller, J. *Computational Materials Science* **1996**, *6*, 15 – 50.

(16) Kresse, G.; Furthmüller, J. *Phys. Rev. B* **1996**, *54*, 11169–11186.

(17) Perdew, J. P.; Burke, K.; Ernzerhof, M. *Phys. Rev. Lett.* **1996**, *77*, 3865–3868.

(18) Blöchl, P. E. *Phys. Rev. B* **1994**, *50*, 17953–17979.

(19) Kresse, G.; Joubert, D. *Phys. Rev. B* **1999**, *59*, 1758–1775.

(20) Hamann, D. R. *Phys. Rev. B* **1997**, *55*, R10157–R10160.

(21) Monkhorst, H. J.; Pack, J. D. *Phys. Rev. B* **1976**, *13*, 5188–5192.

(22) Methfessel, M.; Paxton, A. T. *Phys. Rev. B* **1989**, *40*, 3616–3621.

(23) Ed. Chase, M.; Davies, C.; Downey, J.; Frurip, D.; MacDonald, R.; Syverud, A., *NIST-JANAF Thermodynamical Tables*, Suppl. 1 to Vol 14 of J. Phys. Chem. Ref. Data, 1985; Vol. 14.

(24) Martínez, J. I.; Hansen, H. A.; Rossmeisl, J.; Nørskov, J. K. *Phys. Rev. B* **2009**, *79*, 045120.

(25) Calle-Vallejo, F.; Martnez, J. I.; Garca-Lastra, J. M.; Mogensen, M.; Rossmeisl, J. *Angew Chem Int Edit*, *49*.

(26) Loffreda, D. *Surf. Sci.* **2006**, *600*, 2103 –2112.

(27) Kolb, M. J.; Calle-Vallejo, F.; Juurlink, L. B. F.; Koper, M. T. M. Supporting Information to : Density functional theory study of adsorption of H2O, H, O, and OH on stepped platinum surfaces., `ftp://ftp.aip.org/epaps/journ_chem_phys/E-JCPSA6-140-043413/`, 2014.

(28) Olsen, R. A.; Kroes, G. J.; Baerends, E. J. *J. Chem. Phys.* **1999**, *111*, 11155–11163.

(29) Gudmundsdóttir, S.; Skúlason, E.; Jónsson, H. *Phys. Rev. Lett.* **2012**, *108*, 156101.

(30) Gudmundsdottir, S.; Skulason, E.; Weststrate, K.-J.; Juurlink, L.; Jonsson, H. *Phys. Chem. Chem. Phys.* **2013**, *15*, 6323–6332.

(31) Tritsaris, G.; Greeley, J.; Rossmeisl, J.; Nørskov, J. *Catal. Lett.* **2011**, *141*, 909–913.

(32) Jacob, T.; Muller, R. P.; Goddard, W. A. *J. Phys. Chem. B* **2003**, *107*, 9465–9476.

(33) Feibelman, P. J.; Esch, S.; Michely, T. *Phys. Rev. Lett.* **1996**, *77*, 2257–2260.

(34) Meng, S.; Wang, E. G.; Gao, S. *Phys. Rev. B* **2004**, *69*, 195404.

(35) Vassilev, P.; van Santen, R. A.; Koper, M. T. M. *J. Chem. Phys.* **2005**, *122* 054701.

(36) Karp, E. M.; Campbell, C. T.; Studt, F.; Abild-Pedersen, F.; Nørskov, J. K. *J. Phys. Chem. C* **2012**, *116*, 25772–25776.

(37) Tripković, V.; Skúlason, E.; Siahrostami, S.; Nørskov, J. K.; Rossmeisl, J. *Electrochimica Acta* **2010**, *55*, 7975 –7981.

(38) Van der Niet, M. J. T. C.; Garcia-Araez, N.; Hernández, J.; Feliu, J. M.; Koper, M. T. M. *Catalysis Today* **2013**, *202*, 105 –113.

(39) Lew, W.; Crowe, M. C.; Campbell, C. T.; Carrasco, J.; Michaelides, A. *The Journal of Physical Chemistry C* **2011**, *115*, 23008–23012.